

CROSS-POLARIZATION OPTICAL COHERENCE TOMOGRAPHY IN EVALUATION OF ATHEROSCLEROTIC PLAQUE STRUCTURE

UDC 616.31–018.73–073.756.8:615.831

Received 12.04.2013



E.V. Gubarkova, Junior Researcher, Scientific Research Institute of Biomedical Technologies¹;

M.Yu. Kirillin, PhD, Senior Researcher²;

E.A. Sergeeva, PhD, Senior Researcher²;

E.B. Kiseleva, Junior Researcher, Scientific Research Institute of Biomedical Technologies¹;

L.B. Snopova, D.Bio.Sc., Head of the Morphology Department, Central Scientific Research Laboratory¹;

N.N. Prodanets, PhD, Senior Researcher, the Morphology Department, Central Scientific Research Laboratory¹;

E.G. Sharabrin, D.Med.Sc., Director of Scientific Research Institute of Applied and Fundamental Medicine¹;

E.B. Shakhov, PhD, Head of Division¹;

S.V. Nemirova, PhD, Associate Professor, the Department of Hospital Surgery named after B.A. Korolyov¹;

N.D. Gladkova, D.Med.Sc., Professor, Deputy Director for Science, Scientific Research Institute of Biomedical Technologies, Head of Biotussie Optical Structure Research Laboratory, Scientific Research Institute of Biomedical Technologies¹

¹Nizhny Novgorod State Medical Academy, Minin and Pozharsky Square, 10/1, Nizhny Novgorod, Russian Federation, 603000;

²Institute of Applied Physics of Russian Academy of Sciences, Ul'yanova St., 46, Nizhny Novgorod, Russian Federation, 603155

The cross-polarization optical coherence tomography (CP OCT) technique allows for tissue structure imaging by registration of backscattered radiation in initial and orthogonal polarizations and further comparison of the obtained images. Spatial structure of collagen fibers gives rise not only to backscattering of probing radiation, but also to evolution of its polarization state during propagation through the tissue (depolarization). Collagen fibers of the fibrous cap play a key role in determining the stability of atherosclerotic plaques. Inflammation observed in atherosclerosis is the principal mechanism of collagen fibers disorganization, therefore, the assessment of the depolarizing properties of the fibrous cap can characterize an atherosclerotic plaque as being “vulnerable” to rupture.

The aim of the study was to evaluate CP OCT efficiency to determine the condition of collagen fibers of an atherosclerotic plaque fibrous cap, which characterize its “vulnerability”.

Materials and Methods. 54 *post mortem* samples of intact human aorta and aorta with atherosclerotic plaques at different stages were studied. The study involved 150 CP OCT-images in which the value of OCT signal in orthogonal polarization was used to evaluate the ratio of organized and disorganized by inflammation collagen fibers within the fibrous cap. For histological imaging comparison we used hematoxylin-eosine and picosirius red staining with evaluation in polarized light. Numerical analysis of CP OCT-images was used as a complementary tool for visual assessment.

Results. We showed CP OCT to have significant advantages over the traditional OCT in the assessment of atherosclerotic plaque. In orthogonal CP OCT-image one can differentiate the main structural components of a plaque: a fibrous cap and a lipid core. The thickness of the fibrous cap in the orthogonal polarization image correlates with the thickness of the fibrous cap measured from histological preparations (correlation coefficient $r=0.991$, $p<0.0001$). The integral depolarization factor which characterizes the functional status of collagen fibers of fibrous cap has been used to differentiate the “vulnerable” atherosclerotic plaque. Its value within the range of 0.08–0.12 with 95% probability indicates low content of highly organized collagen in the fibrous cap, and hence, its tendency to rupture.

Conclusion. CP OCT is capable of assessing the functional state of collagen fibers of fibrous cap of an atherosclerotic plaque with high probability. Numerical analysis of CP-OCT images provides identification of “vulnerable” atherosclerotic plaques.

Key words: cross-polarization optical coherence tomography; CP OCT; atherosclerotic plaques; “vulnerable” atherosclerotic plaques; OCT signal numerical processing.

For contacts: Gladkova Nataliya Dorofeevna, phone: +7951-910-66-57; e-mail: natalia.gladkova@gmail.com

Currently, optical coherence tomography (OCT) is recognized by world community as an innovative medical diagnostic technique used for imaging internal structure of human tissues. OCT technique allows to obtain high-contrast two- and three-dimensional images of tissue structure at depth up to 1–2 mm with micron resolution (up to 3 μm) in real time. The technique is based on low-coherence interferometry of infrared radiation (700–1300 nm). OCT has significant advantages as a technique capable to obtain images of internal organs and use endoscopic probes including intravascular ones [1, 2].

Back in 1991, the OCT inventors supposed that OCT can be used for imaging atherosclerotic process in vessels [3] being an alternative or a supplementary tool to intravascular ultrasound (IV US) [4]. In contrast to ultrasonic technique, in which an echo signal caused by spatial distribution of acoustic impedance is recorded, OCT detects light backscattered from optical inhomogeneities, resulting in at least 10 times higher OCT spatial resolution compared to that of US [1].

Recently, dramatic advance has been made in the development of a new OCT modality based on spectral interferometry and referred to as frequency-domain OCT (or spectral domain OCT). It enables high-speed imaging, including video mode [5]. Imaging speed of the last-generation OCT devices has reached 3000–4000 frames per second [6] providing the possibility to obtain an OCT-image at the moment of radiopaque contrast (clearing) agent passing through a vessel lumen, and visualize the atherosclerotic plaque structure [4, 7–9].

Later the possibility to obtain IV OCT-images without proximal balloon occlusion of a vessel was achieved using the isomolar contrast agent iodixanol injected from a special introducer [10]. This approach is applied in combination with spectral OCT and intravascular imaging system C7XR (ImageWire; LightLab Imaging, Inc., USA) [11].

IV OCT is a high-potential technique in stenting monitoring, as well as in early detection of complications related to stenting, such as incomplete stent opening and intimal dissection [12–14]. Compared to angiography and IV US, IV OCT provides more accurate data on rate of neointimal hyperplasia on stent strata and features of morphological changes in atherosclerotic plaques in restenosis after stenting depending on stent types [15].

One of the critical challenges for IV OCT is the diagnosis of a “vulnerable” atherosclerotic plaque. R. Virmani et al. [16] suggested determining the “vulnerability” of plaques resulting in acute coronary syndrome based on the thickness of its fibrous cap. The authors demonstrated the thickness of fibrous caps prone to rupture to be $23 \pm 19 \mu\text{m}$, and fibrous cap thickness less than 64 μm to be critical with a probability of 95% (within the limits of two standard deviations). IV US has spatial resolution of 80–90 μm [4]. Consequently, this technique fails to detect fibrous cap thickness less than 65 μm . OCT spatial resolution is not worse than 20 μm enabling to detect a thin fibrous cap of an atherosclerotic plaque.

The experience of IV OCT application in cardiology has showed the efficiency of three *in vivo* OCT-markers of atherosclerotic plaque: fibrous cap thickness, concentration

of macrophages/foam cells and a plaque type: fibrous, fibro-calcific and lipid. The first marker, the thickness of fibrous cap, is recognized as indisputable, and its significance was demonstrated by many researchers [5, 17–19]. However, recently, an opinion that the contrast of the fibrous cap and a lipid core is not always sufficient to define fibrous cap borders in OCT-image has been proposed [20]. The second marker is the concentration of macrophages in the fibrous cap of an atherosclerotic plaque [21, 22]. The approach described by G.J. Tearney and B.E. Bouma is confirmed and being developed, though having its opponents [20, 23]. The third OCT-marker originates from the possibility to differentiate fibrous, fibro-calcific and lipid-rich plaque in OCT-image [24]. The features of three types of plaques were specified, although causing a high error level in detection of a plaque with the fibrous cap and a lipid core (sensitivity 71–79%) due to low contrast of the structures in OCT-image [20].

The content of highly organized type I collagen in fibrous cap determines structural stability of an atherosclerotic plaque. In a thin-walled plaque the presence of metalloproteases synthesized by inflammatory cells, lead to the exhaustion of type I collagen. The result is a mechanically “vulnerable” plaque wall. Detection of a “vulnerable” atherosclerotic plaque remains difficult for standard OCT, since the lower border of fibrous cap is not always distinguished from lipid core due to similar optical properties, what prevents reliable measurements of fibrous cap thickness [20].

The border between a fibrous cap and lipid tissue can be detected by means of polarization sensitive OCT (PS-OCT), which in addition to a standard OCT-image provides a phase retardation map [19, 25–28], which in-depth rate of change characterizes the organization degree of proteins and macromolecules, such as collagen and actin [29–31]. The increase in the in-depth rate of phase retardation change in PS OCT-images implies the increase in atherosclerotic plaque stability [28]. However, the implementation of intravascular PS OCT technique in clinical practice is intricate due to a number of technical problems related to the maintenance of light polarization in a fiber when using a rapidly rotating catheter. Recently, several solutions to these problems have been suggested [32–36]. Pilot studies are being carried out using intravascular PS OCT in patients [37]. If successful, intravascular PS OCT can give additional information on structural integrity of coronary arteries [38].

Cross-polarization OCT (CP OCT) is a modification of PS OCT, which simultaneously forms two images by separate detection of scattered radiation in two channels, parallel and orthogonal to polarization of probing radiation. Unlike PS OCT, which inspects birefringent properties of the tissue under study manifested by patterns of phase retardation maps, CP OCT allows imaging of radiation depolarization both due to birefringence and scattering in biological tissue [39]. First CP OCT devices were described and used by our team for dental tissue imaging [40], and later for *in vivo* studies of mucosa of internal organs [41]. A group of J.M. Schmitt used CP OCT to study phantom media and skin [39]. The comparison of backscattered patterns in initial and orthogonal polarization appeared to be more

informative compared to the analysis of phase retardation maps for biological tissues with low birefringence, in which organized collagen fibers do not have regular in-depth structure (anisotropic tissues, including mucosa of internal organs as well as arterial vessels) [42, 43]. We have failed to find any paper dealing with atherosclerotic plaque studies using CP OCT.

The aim of the study was to evaluate CP OCT efficiency to determine the state of collagen fibers of an atherosclerotic plaque fibrous cap, which characterize its “vulnerability”.

Materials and Methods. The subjects of CP OCT-study were *post mortem* specimens of the human aorta with atherosclerotic plaques at different atherosclerotic stages. In obtained CP OCT-images we evaluated the ratio of organized and disorganized by the inflammation collagen fibers within a fibrous cap by the value of OCT signal in orthogonal polarization.

54 specimens of aortic vessels were studied including 5 specimens of intact aortic tissue of a patient died from diseases unrelated to vascular pathology, without atherosclerotic signs (18-year-old male cadaver) and 49 specimens of pathologically changed aortic wall tissue with atherosclerotic signs from patients died of cardiovascular diseases (2 male and 5 female cadavers aged 60–75). Total amount of 150 CP OCT-images were obtained and analyzed.

Thoracic aortic specimens were obtained less than 24 h post mortem, separated from perivascular tissues, cut into fragments, 5–7 mm in length, and delivered in gauze saturated with phosphate buffer at 4°C. To minimize the effect of post mortem changes, the samples were studied during first 2 hours after excision. For proper orientation of tissues section during histology ink marks we placed on upper, lower, proximal and distal ends on the adventitia side of the specimens under study.

In this study we employed CP OCT system “OCT 1300-U” developed at the Institute of Applied Physics of RAS (“BioMedTech Ltd”, Nizhny Novgorod, Russia) [44, 45] equipped with en-face endoscopic probe of 2.7 mm in outer diameter. The device employs probe radiation with the wavelength of 1300 nm and power of 3 mW; axial resolution is 15 μm in free space, transversal resolution resolution is 25 μm. The system simultaneously demonstrates two conjugate images: in initial and orthogonal polarizations with strict spatial correspondence of image pixels. Each CP OCT-image has a size of 2x2.4 mm and is obtained at a rate of 0.5 fps [44].

Each vascular fragment was placed on a plane surface and inspected by CP OCT from the intimal side (Fig. 1, a). OCT-probe was successively shifted along a vessel ensuring overlapping of the neighboring CP OCT-images (provided that the width of scanning area is less than the outside diameter of a probe) in two lines 4 mm away from the section edge that enabled to obtain a continuous OCT-image of a larger area and further perform a “target” histologic study (Fig. 1, b).

After CP OCT-scanning a tissue fragment was excised, fixed in 10% formalin solution, dehydrated in high-proof alcohol, and embedded in paraffin. Histological sections, 7 μm in thickness, were prepared with sledge microtome

Leica SM2000R (Leica Microsystems, Germany). The material was histologically evaluated using light microscopy and hematoxylin-eosine staining providing a general idea of morphological changes, and using a specific histological staining by picrosirius red (PSR) with microscopic estimation in crossed polarizers to study collagen fibers (Leica DFC245 C microscope; Leica Microsystems, Germany). Such staining is the most recognized method of morphological assessment of collagen fiber condition (the degree of their organization, size, amount, mutual arrangement of fibers and its birefringence ability) that enables to assess functional state of collagen fibers [46]. PSR chemically reacts with collagen, so organized collagen fibers in polarized light appear as bright areas. Yellow-orange and red colors are typical for organized thick collagen fibers (type I collagen, fibers are 1–3 μm in diameter), and deep green color for thin fibers (type III collagen, fibers are 0.8 μm in diameter). Completely disorganized collagen fibers do not exhibit luminescence.

The results were assessed in two stages. The first stage aimed at visual estimation of CP OCT-images of atherosclerotic plaques accounting their stages by

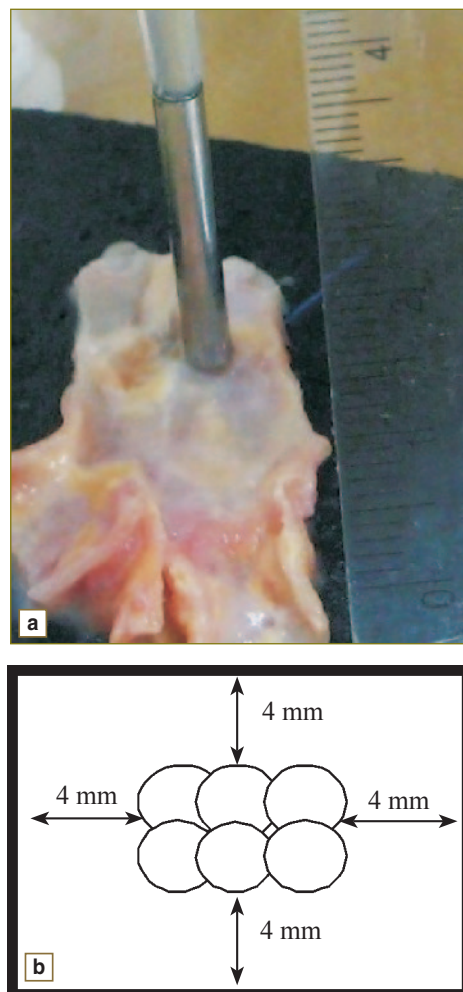


Fig. 1. CP OCT examination of aortic tissue samples: a — the position of the probe when scanning an inner surface of aortic wall, b — OCT-scanning scheme

comparing them with histological images. The second stage included numerical OCT-signal processing in both polarizations according to two parameters: the thickness of fibrous cap and the ratio of signals in initial and orthogonal polarizations.

The first assessment stage. For verification of structures on CP OCT-images we used digital photos of histological sections, with frame size comparable with scan area size. Basing on visual estimation of the histological images of atherosclerotic plaques, we formed groups of images for each clinical case including CP OCT-image and corresponding images of histological sections with different staining.

We studied 49 human aortic specimens with atherosclerotic signs and separated them into atherosclerotic plaque stages according to American Heart Association criteria [47] and “vulnerability” criteria according to R. Virmani [16]:

stage II of atherosclerotic plaque: deposits of foam cells and lipid-coated smooth muscle cells with no extracellular lipids and pathological intimal thickening — 8 specimens;

stage III (intermediate): besides foam cells a small amount of extracellular lipid inclusions are present; a fibrous cap is formed predominantly by type I collagen fibers — 10 specimens;

stage IV (true atheroma): the presence of lipid core and fibrous cap, in which type I collagen fibers are partially replaced by type III collagen fibers or disorganized due to proteolytic enzyme action — 10 specimens;

stage V: lipid core, distinct fibrous connective tissue layers (collagen fibers in different state) — 21 specimens:

stage Va: a distinct lipid core covered by one or several fibrous layers (“vulnerable” atherosclerotic plaque) — 8 specimens;

stage Vb: fibroatheroma with calcinosis — 5 specimens;

stage Vc: fibroatheroma with a manifestative fibrous cap irregular in thickness and a minimal lipid core — 8 specimens.

The second assessment stage included two procedures:

1. The measurement of intimal thickness of intact wall or fibrous cap of aortic atherosclerotic plaque from CP OCT-images; thickness value was compared with that of the same structures from histological specimens.

To measure fibrous cap thickness in CP OCT-images we used ImageJ program (National Institute of Health, Washington, USA) enabling to determine the distance between the selected points in an image. We considered the part of fibrous cap of the atherosclerotic plaque with the smallest thickness in the selected area. Thickness was measured as the vertical distance between the upper and lower borders of the area orthogonal OCT-image which histologically corresponded to organized collagen fibers.

For PSR and hematoxylin-eosin stained histological specimens the thickness of fibrous cap was the vertical distance between its upper and lower borders. The thickness of fibrous cap was estimated at stages IV, Va and Vc of an atherosclerotic plaque with a well shaped fibrous cap. Intimal thickness of intact aortic wall, which in norm is 5–15 μm and is presented by a high-level OCT-signal from

the internal elastic membrane was considered as a control value [48]. The thickness was assessed in the following groups: 1) tissue of intact aortic wall (control); 2) an atherosclerotic plaque, stage IV — aorta with a thick regular fibrous cap (over 65 μm) above a distinct lipid core; 3) an atherosclerotic plaque, stage Va — aorta with a thin fibrous cap (below 65 μm); 4) an atherosclerotic plaque, stage Vc — aorta with a thick fibrous cap, irregular in thickness (above 65 μm) and minimal lipid core.

2. To estimate depolarization properties of the tissues under study we used an original approach: calculation of integral depolarization factor (IDF) [49]. IDF is a dimensionless parameter, which was calculated as an averaged ratio of the OCT-signals registered in orthogonal and initial polarizations:

$$IDF = \frac{1}{N} \sum_{i=1 \dots N, P_i^\perp > \langle P_{noise} \rangle + 2s_{noise}} \frac{P_i^\perp - \langle P_{noise} \rangle}{P_i^\parallel}$$

where: P_i^\parallel is the OCT-signal in initial polarization for i -th pixel after averaging over transverse coordinate; P_i^\perp is the OCT-signal in orthogonal polarization for i -th pixel after averaging over transverse coordinate; N is the number of pixels in averaged over transverse coordinate OCT-signal in orthogonal polarization, for which the OCT-signal exceeds average noise level $\langle P_{noise} \rangle$ by a doubled standard deviation of noise level $2s_{noise}$.

IDF calculation accounts for the key features of CP OCT-image formation and is not affected by speckle noise and instrumental noise. IDF enables to characterize numerically the tissue ability to depolarize polarized probing light wave, and thus evaluate functional state of the collagen-containing tissue under study. We used an original automatic IDF calculation program [49].

When estimating the intensity of luminescence in polarized light for red zones of PSR stained histological specimens (type I collagen fibers), we chose the image areas corresponding to those in orthogonal CP OCT-images. The values of intensity of luminescence were averaged over rectangular areas corresponding to fibrous cap position in orthogonal CP OCT-image.

Spearman correlation coefficient was calculated: a) between the thickness of fibrous cap in orthogonal CP OCT-images and that for PSR stained histological specimens; b) between the IDF values for CP OCT-images and the intensity of luminescence of collagen fibers for PSR stained histological specimens (for each stage of atherosclerotic process). Taking into account the small number of images in considered groups, we used non-parametric Mann–Whitney test to calculate statistical significance of differences. Mean values were presented as $M \pm SD$, where M is arithmetic mean, and SD is standard deviation.

Results and Discussion.

The first assessment stage. Comparative visual analysis of 150 CP OCT-images in initial and orthogonal polarizations and histological specimens with different staining showed the following:

1. Intact aortic tissue consisting predominantly of elastic

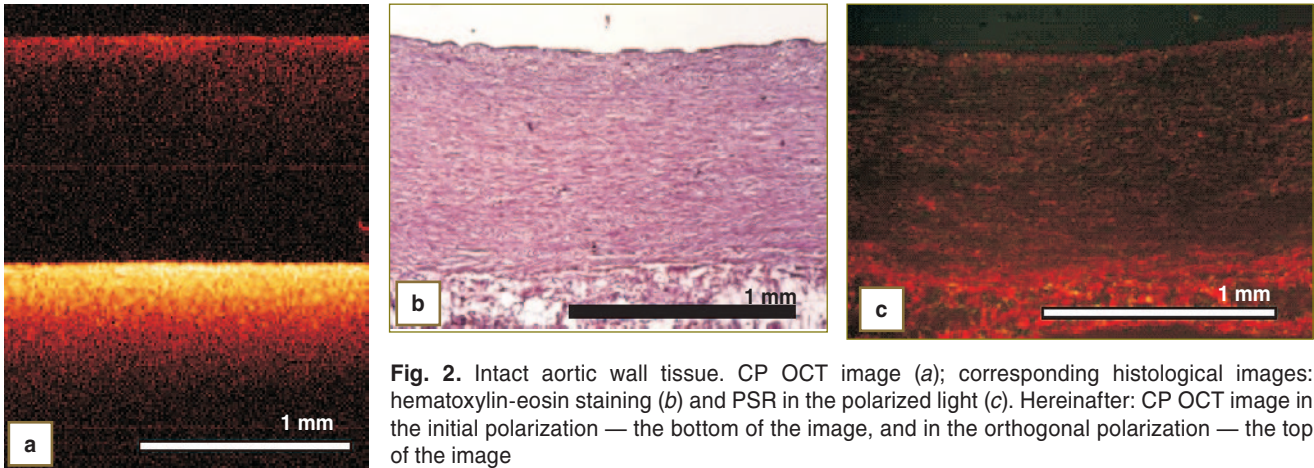


Fig. 2. Intact aortic wall tissue. CP OCT image (a); corresponding histological images: hematoxylin-eosin staining (b) and PSR in the polarized light (c). Hereinafter: CP OCT image in the initial polarization — the bottom of the image, and in the orthogonal polarization — the top of the image

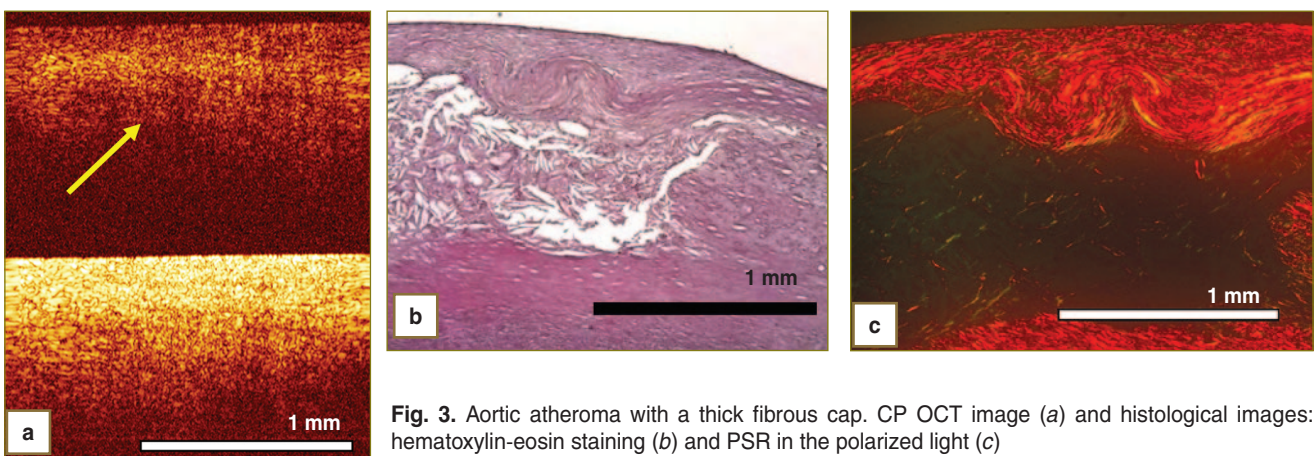


Fig. 3. Aortic atheroma with a thick fibrous cap. CP OCT image (a) and histological images: hematoxylin-eosin staining (b) and PSR in the polarized light (c)

membranes, smooth muscular fibers and a few type III collagen fibers (Fig. 2, b, c) results in strong backscattering of probing radiation in initial polarization, and weak backscattering in orthogonal polarization (Fig. 2, a). CP OCT-images have high uniformly attenuating signal in initial polarization; and low signal in orthogonal polarization indicating weak tissue ability to depolarize radiation (lack of type I collagen).

2. Atherosclerotic plaque, stage IV (true atheroma) is characterized morphologically by the presence of lipid necrotic core and fibrous cap, in which organized type I collagen fibers prevail together with presence of collagen fibers disorganized by inflammation (Fig. 3, b, c). In CP OCT-image in initial polarization the signal level is higher compared to intact aortic wall tissue due to the presence of type I collagen in the cap, the OCT-signal attenuates in the area of lipid core, and the contrast of the border of these structures is low (not more than 3 dB). In orthogonal polarization lipid core is manifested by the area with low signal level below the fibrous cap of the plaque characterized by high signal level: the contrast of the border of lipid core and fibrous cap (arrow) is significantly higher than that in initial polarization (over 8 dB) (Fig. 3, a).

3. Atherosclerotic plaque, stage Va: a plaque includes a distinct lipid core covered by a thin fibrous cap (Fig. 4, b, c). In OCT-image in orthogonal polarization the areas of a

thin fibrous cap of an atherosclerotic plaque ($59 \pm 9 \mu\text{m}$ in thickness) are present above the lipid core corresponding to “vulnerability” criterion according to R. Virmani (Fig. 4, a). The contrast of the border between the fibrous cap and a lipid core in OCT-images in orthogonal polarization is sufficient (not less than 6 dB) to measure the thickness of a fibrous cap in contrast to initial polarization to measure the same one.

4. Atherosclerotic plaque, stage Vc is fibroatheroma with a very thick fibrous cap and weakly manifested lipid core (Fig. 5, b, c). In OCT-image in initial polarization the OCT-signal exceeds the noise level throughout the whole image depth; in the image two zones are distinguished: the upper one is characterized by high level and low attenuation of the OCT-signal, and the lower one — by low signal level and the presence of the structure supposedly corresponding to a bundle of collagen fibers (Fig. 5, a). Such atherosclerotic plaque is usually referred to as “stable”, since its fibrous cap safely separates a necrotic core from the vessel lumen. Lipid core in CP OCT-images is actually unseen, since it is outside the image area (deeper than 1 mm).

In particular cases in CP OCT-image in orthogonal polarization accumulations of calcium crystals are clearly manifested as bright formations, predominantly round-shaped, in the fibrous cap area, which form an optical “shadow” behind them (Fig. 6, a).

The considered cases allow to suppose that CP OCT

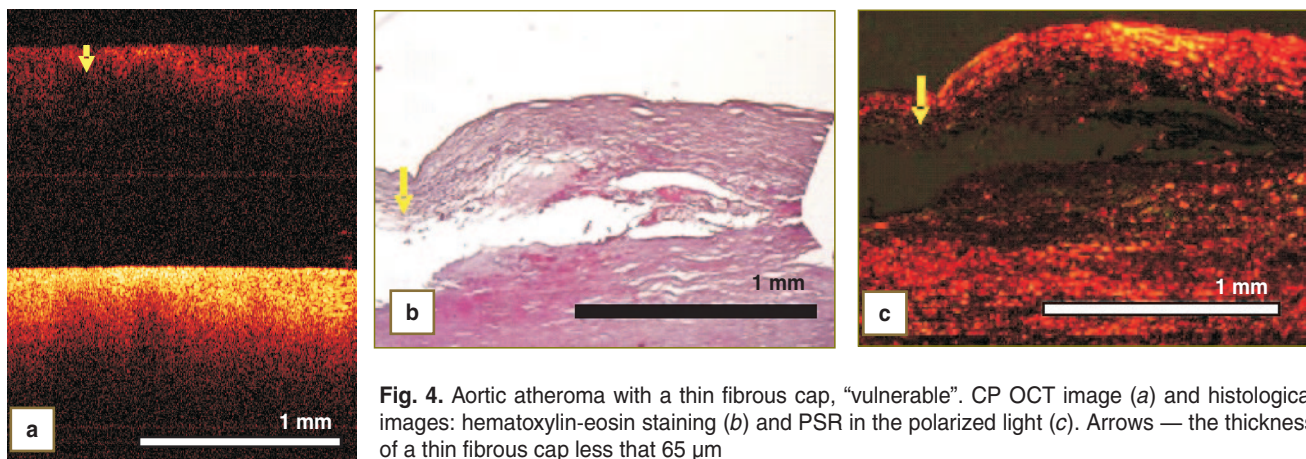


Fig. 4. Aortic atheroma with a thin fibrous cap, “vulnerable”. CP OCT image (a) and histological images: hematoxylin-eosin staining (b) and PSR in the polarized light (c). Arrows — the thickness of a thin fibrous cap less that 65 μ m

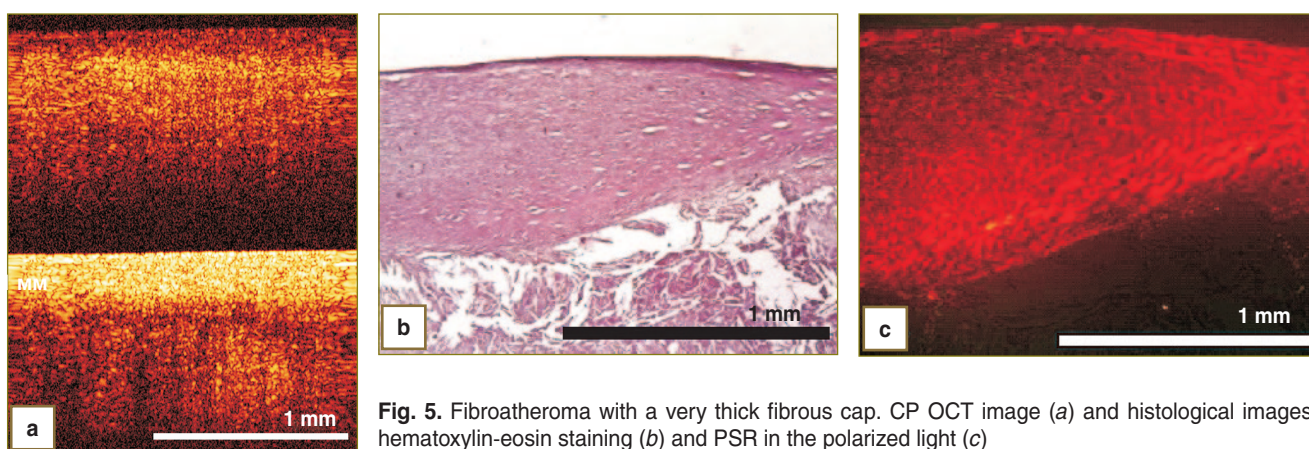


Fig. 5. Fibroatheroma with a very thick fibrous cap. CP OCT image (a) and histological images: hematoxylin-eosin staining (b) and PSR in the polarized light (c)

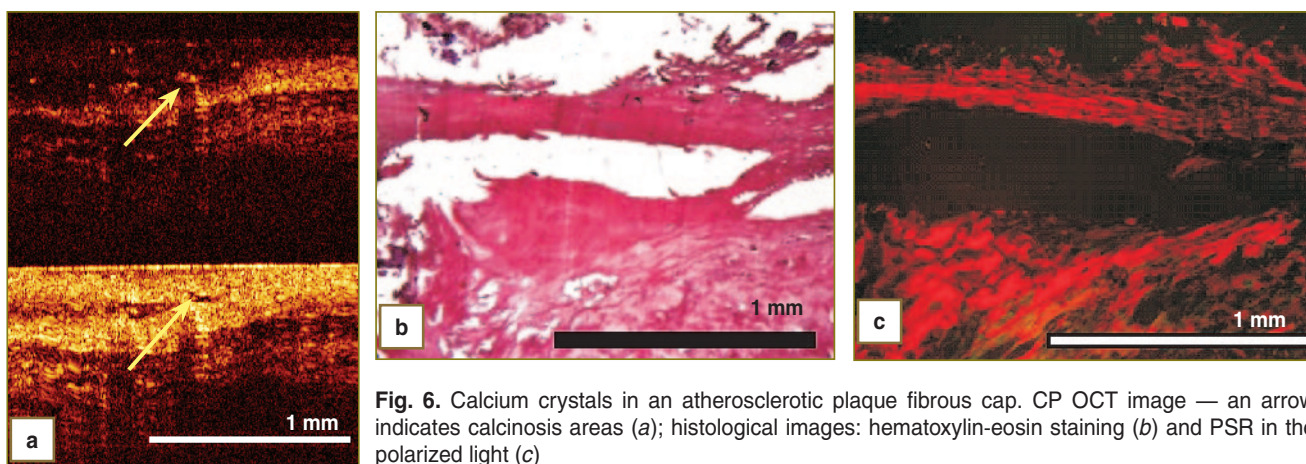


Fig. 6. Calcium crystals in an atherosclerotic plaque fibrous cap. CP OCT image — an arrow indicates calcinosis areas (a); histological images: hematoxylin-eosin staining (b) and PSR in the polarized light (c)

enables to differentiate the condition of collagen fibers in the fibrous cap of an atherosclerotic plaque by analysis of OCT-signal in the orthogonal polarization. The study of luminescence of collagen fibers in histological specimens with PSR staining in polarized light showed organized type I collagen to give rise to bright red luminescence, while disorganized collagen produces no luminescence. Basing on results of the study we formulated visual attributes of an atherosclerotic plaque in CP OCT-images. Comparative *visual analysis* of 150 CP OCT-images in initial and orthogonal polarizations with histological data

showed that CP OCT enables to distinguish intact aortic wall tissue area from an atherosclerotic plaque, as well as to differentiate its main structural components: lipid core and fibrous cap (See Fig. 3, 4, 5, 6). The border contrast between fibrous cap and lipid core in orthogonal OCT-image of an atherosclerotic plaque is sufficient to measure the thickness of fibrous cap to detect “vulnerable” plaques (Fig. 4), which is an important factor for distinguishing patients with high risk of sudden cardiac arrest.

The second assessment stage. Numerical analysis of OCT-signal in orthogonal images was used as a

supplementary tool to visual assessment of images. In a number of cases this approach is able to increase significantly diagnostic capabilities of CP OCT technique in the assessment of vascular wall condition in atherosclerosis. Two values were assessed: a) the thickness of pathologically changed fibrous cap of an atherosclerotic plaque in orthogonal polarization in various atherosclerotic stages; b) IDF of CP OCT-images. The thickness of the fibrous cap measured from CP OCT-images was compared with the parameters of histological specimens.

No significant difference of fibrous cap thickness of an atherosclerotic plaque was found for histological specimens with various staining (hematoxylin-eosin and PSR) ($p=0.9$, Mann–Whitney test). Therefore, subsequently, for comparison of the fibrous cap thickness in CP OCT-images we used the measurement data of the fibrous cap thickness from PSR stained histological specimens.

The intimal thickness measurement of the intact aortic wall and the fibrous cap of an atherosclerotic plaque in CP OCT-images in orthogonal polarization was possible, since border contrast of the fibrous cap and lipid core was sufficient. In addition, in initial polarization the signal covered a significantly larger image area, and in 10 images (33.3% of cases) it exceeded the noise level throughout the image depth that enabled to accurately determine the fibrous cap thickness. Thus, we used the measurement of the fibrous cap thickness only in the orthogonal polarization, since in initial polarization the border was not distinguishable seen, and compared it with the fibrous cap thickness measurement from PSR stained histological specimens (Table 1, Fig. 7).

The thickness of the fibrous cap of “vulnerable”

Table 1

Fibrous cap thickness in groups with various stages of the aortic atherosclerotic plaque

Statistical values	Intact wall	Stage IV	Stage Va	Stage Vc
PSR staining, M±SD, μm	12±8	540±24	63±7	785±34
CP OCT images, M±SD, μm	12±8	496±25	59±9	760±30
Number of images	7	8	8	7
Spearman rank correlation*	1.00; $p=0.01$	0.81; $p=0.01$	0.90; $p=0.001$	0.89; $p<0.05$
Mann–Whitney test**	$p>0.05$	$p>0.05$	$p>0.05$	$p>0.05$

* — Spearman correlation coefficient between the fibrous cap thickness on CP OCT images and PSR specimens in a general group of samples without grouping them by stages was 0.991 ($p<0.0001$); ** — significance level of difference between fibrous cap thickness on CP OCT-images and PSR specimens, $p>0.05$ (Mann–Whitney test).

atherosclerotic plaques (stage Va) was found to be $59\pm 9\ \mu\text{m}$, being significantly lower than for atherosclerotic plaque at stage IV ($496\pm 25\ \mu\text{m}$) and Vc ($760\pm 30\ \mu\text{m}$) (Fig. 7). We determined statistically significant difference of the fibrous cap thickness of the atherosclerotic plaque at stages under study from its values at stage Vc, $p=0.002$, as well as between the stages IV and Va of an atherosclerotic plaque, $p=0.0001$ (Mann–Whitney u-test).

In each of the groups divided according to the stages of an atherosclerotic plaque we calculated the correlation coefficient between the fibrous cap thickness in the orthogonal polarization and PSR stained histological specimens (See Table 1). No significant differences in the fibrous cap thickness were found ($p>0.05$, Mann–Whitney test).

We revealed high correlation of the fibrous cap thickness measured in orthogonal images and histological specimens for all atherosclerotic plaque stages under study ($r=0.81\text{--}1.00$; $p<0.05$, Table 1), while the fibrous cap thickness of an atherosclerotic plaque in orthogonal images for all considered cases (without division according to atherosclerotic plaque stages) correlates with the fibrous cap thickness measured from histological specimens

Fig. 7. Fibrous cap thickness in groups with different stages of the aortic atherosclerotic plaques on CP OCT images in the orthogonal polarization and histological specimens stained by PSR; * — statistically significant difference of values with orthogonal OCT image series with Vc stage plaque, $p<0.01$ (Mann–Whitney test); ** — statistically significant difference of values with histological specimen series with Vc stage plaque, $p<0.01$ (Mann–Whitney test)

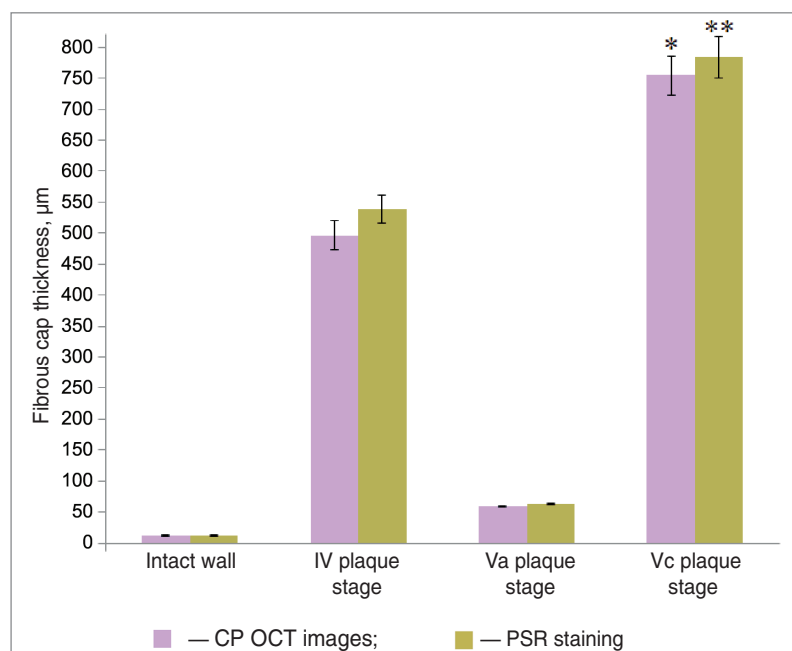


Table 2

Integral depolarization factor in groups with various stages of the aortic atherosclerotic plaque

Statistical values	Intact wall	Stage IV	Stage Va	Stage Vc
M±SD	0.06±0.01	0.21±0.01**	0.10±0.01**	0.24±0.01*
Number of images	7	8	8	7
95% CI	0.04–0.08	0.15–0.27	0.12–0.08	0.32–0.16

* — statistically significant differences of the IDF values atherosclerotic plaque values at different stages from the intact aortic tissue IDF, $p=0.01$ (Mann–Whitney test);
 + — statistically significant difference of the IDF values of stage IV (atheroma) and Va stage (“vulnerable” plaque) of the atherosclerotic plaque, $p<0.01$ (Mann–Whitney test);
 95% CI — confidence interval of 95% probability.

($r=0.991$; $p<0.0001$, Table 1). Thus, we can conclude that OCT-signal in an orthogonal image enables to identify the condition of collagen fibers of the fibrous cap, including the plaques with fibrous cap thickness below 65 μm . This ensures a certain advantage of the technique: ability for *in vivo* detection of an unstable atherosclerotic plaque.

“Vulnerability” of an atherosclerotic plaque is determined not only by a small thickness of the fibrous cap, but also by the disorganization degree of its collagen fibers [20]. As we mentioned above, OCT-signal in the orthogonal image is produced by highly organized type I collagen, which can depolarize probing radiation. For objective assessment of OCT-signal in orthogonal images and development of a criterion for differential diagnostics of various stages of atheromas with the fibrous cap above a contrast lipid core (atherosclerotic plaque stages IV, Va and Vc) we calculated IDF values for different groups of images (Table 2).

IDF value for intact aortic wall tissue was 0.06 ± 0.01 , the lowest level among all the considered groups. Increase IDF relative to intact aortic wall tissue indicates the improvement of depolarization properties of aortic wall due to the appearance of organized type I collagen in it. Depending on the stage of an atherosclerotic plaque, the thickness of a fibrous cap may vary. IDF value was found to increase up to 0.21 ± 0.01 , in case of the fibrous cap thickness of 450–600 μm , and

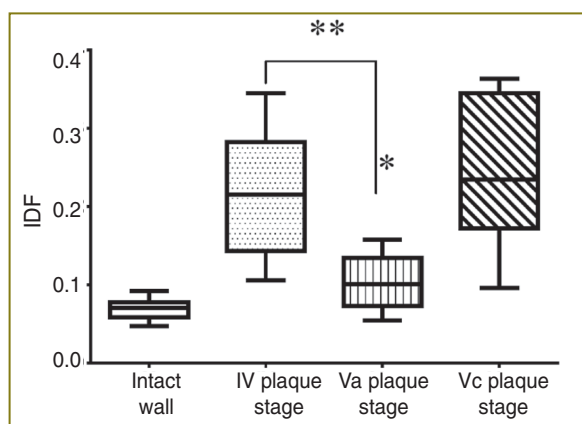


Fig. 8. IDF of CP OCT images of the intact wall and IV, Va, Vc stages of the aortic atherosclerotic plaque; * — statistically significant difference with the intact aortic wall, $p=0.01$ (Mann–Whitney test); ** — statistically significant difference between stages IV and Va, $p<0.01$ (Mann–Whitney test)

0.24 ± 0.01 for fibrous cap thickness of 700–800 μm . Disorganization of collagen fibers due to a pronounced inflammatory process in a vascular wall results in the fibrous cap thinning, with IDF decreasing down to 0.10 ± 0.01 , though remaining statistically significantly higher than that in intact aortic wall tissue.

IDF for “vulnerable” plaques (stage Va) cases among the atherosclerotic stages under study was 0.10 ± 0.01 and appeared to be statistically significantly higher than at atherosclerotic plaque stage IV (0.22 ± 0.01), which had a fibrous cap of thickness above 65 μm

(See Fig. 5). The 95% confidential interval of IDF values for a “vulnerable” plaque was 0.08–0.12 (within the limits of two standard deviations). Automatic detection of this factor in CP OCT-study of the arterial wall can indicate the risk of appearing fibrous cap area ready to rupture (Fig. 8).

Spearman correlation coefficient between IDF and luminescence intensity of collagen fibers in PSR stained histological specimens was 0.478 ($p<0.05$), which means that experimental data do not contradict the hypothesis that IDF correlates with PSR luminescence intensity with 95% probability.

Thus, IDF provides significant supplementary information on condition of collagen fibers of fibrous tissue *in vivo* and is able to reveal the atherosclerotic plaque rupture risk.

Conclusion. Cross-polarization optical coherence tomography (CP OCT) has significant advantages over traditional OCT in the assessment of the atherosclerotic plaque condition. In orthogonal OCT-image of the atherosclerotic plaque in orthogonal its main structural components — a fibrous cap and a lipid core — are clearly distinguished.

The thickness of the atherosclerotic plaque fibrous cap measured in orthogonal OCT-images correlates with the thickness of the fibrous cap measured from histological specimens (Spearman correlation coefficient = 0.991; $p<0.001$).

Integral depolarization factor (IDF) characterizes the functional state of the fibrous cap collagen fibers and can be used for reliable detection of a “vulnerable” atherosclerotic plaque. Its value within the range of 0.08–0.12 indicates low content of organized collagen in the fibrous cap with 95% probability, which may point towards plaque tendency to rupture.

Study Funding. The work was supported by Federal Target Program “Scientific and academic and teaching staff of innovative Russia” (Agreements No.8145 and 8741), Grants of Government of the Russian Federation (Contracts No.11.G34.31.0017 and 14.B25.31.0015).

Conflict of Interest. The authors have no conflict of interests to disclose.

References

1. *Rukovodstvo po opticheskoy kogerentnoy tomografii* [Handbook of optical coherence tomography]. Pod red. Gladkovoy N.D.,

Shakhovoy N.M., Sergeeva A.M. [Gladkova N.D., Shakhova N.M., Sergeev A.M. (editors)]. Moscow: Fizmatlit; 2007; 296 p.

2. Brezinski M.E. Optical coherence tomography. *Principles and applications*. 2 ed; Elsevier; 2013.

3. Huang D., Swanson E.A., Lin C.P., Schuman J.S., Stinson W.G., Chang W., Hee M.R., Flotte T., Gregory K., Puliafito C.A. Optical coherence tomography. *Science* 1991 Nov 22; 254(5035): 1178–1181.

4. Jang I.K., Bouma B.E., Kang D.H., Park S.J., Park S.W., Seung K.B., Choi K.B., Shishkov M., Schlendorf K., Pomerantsev E., Houser S.L., Aretz H.T., Tearney G.J. Visualization of coronary atherosclerotic plaques in patients using optical coherence tomography: comparison with intravascular ultrasound. *J Am Coll Cardiol* 2002 Feb 20; 39(4): 604–609.

5. Brezinski M.E. Optical coherence tomography for identifying unstable coronary plaque. *Int J Cardiol* 2006 Feb 15; 107(2): 159–170.

6. Choi D.-H., Hiro-Oka H., Shimizu K., Ohbayashi K. Spectral domain optical coherence tomography of multi-MHz A-scan rates at 1310 nm range and real-time 4D-display up to 41 volumes/second. *Biomed Opt Express* 2012 Dec 1; 3(12): 3067–3086.

7. Brezinski M., Saunders K., Jessor C., Li X., Fujimoto J. Index matching to improve OCT imaging through blood. *Circulation* 2001 Apr 17; 103(15): 1999–2003.

8. Jang I.K., Tearney G.J., MacNeill B., Takano M., Moselewski F., Iftimia N., Shishkov M., Houser S., Aretz H.T., Halpern E.F., Bouma B.E. In vivo characterization of coronary atherosclerotic plaque by use of optical coherence tomography. *Circulation* 2005 Mar 29; 111(12): 1551–1555.

9. Yamaguchi T., Terashima M., Akasaka T., Hayashi T., Mizuno K., Muramatsu T., Nakamura M., Nakamura S., Saito S., Takano M., Takayama T., Yoshikawa J., Suzuki T. Safety and feasibility of an intravascular optical coherence tomography image wire system in the clinical setting. *Am J Cardiol* 2008 Mar 1; 101(5): 562–567.

10. Prati F., Cera M., Ramazzotti V., Imola F., Giudice R., Albertucci M. Safety and feasibility of a new non-occlusive technique for facilitated intracoronary optical coherence tomography (OCT) acquisition in various clinical and anatomical scenarios. *EuroIntervention* 2007 Nov; 3(3): 365–370.

11. Tearney G.J., Waxman S., Shishkov M., Vakoc B.J., Suter M.J., Freilich M.I., Desjardins A.E., Oh W.Y., Bartlett L.A., Rosenberg M., Bouma B.E. Three-dimensional coronary artery microscopy by intracoronary optical frequency domain imaging: first-in-man experience. *JACC Cardiovasc Imaging* 2008; 1: 752–761.

12. Bezerra H.G., Guagliumi G., Valescchi O. Unraveling the lack of neointimal hyperplasia detected by intravascular ultrasound using optical coherence tomography: lack of spatial resolution or a true biological effect? *J Am Coll Cardiol* 2009; 10(Suppl A): 90A.

13. Finn A.V., Joner M., Nakazawa G., Kolodgie F., Newell J., John M.C., Gold H.K., Virmani R. Pathological correlates of late drug-eluting stent thrombosis: strut coverage as a marker of endothelialization. *Circulation* 2007; 115(18): 2435–2441.

14. Gladkova N.D., Gubarkova E.V., Sharabrin E.G., Stelmashok V.I., Beimanov A.E. Vozmojnosti i ogranichenia vnutrisudistoi opticheskoy kogerentnoy tomografii [The Potential and limitations of intravascular optical coherence tomography]. *Sovrem Tehnol Med — Modern Technologies in Medicine* 2012; 4: 128–141.

15. Terashima M., Kaneda H., Suzuki T. The role of optical coherence tomography in coronary intervention. *Kor J Intern Med* 2012; 27: 1–12.

16. Virmani R., Kolodgie F.D., Burke A.P., Farb A., Schwartz S.M. Lessons from sudden coronary death: a comprehensive morphological classification scheme for atherosclerotic lesions. *Arterioscler Thromb Vase Biol* 2000; 20(5): 1262–1275.

17. Honda Y., Fitzgerald P.J. New Drugs and Technologies. Frontiers in Intravascular Imaging Technologies. *Circulation* 2008 Apr 15; 117(15): 2024–2037.

18. Langer H.F., Haubner R., Pichler B.J., Gawaz M. Radionuclide Imaging: a molecular key to the atherosclerotic plaque. *J Am Coll Cardiol* 2008 Jul 1; 52(1): 1–12.

19. Nadkarni S.K., Bouma B.E., de Boer J., Tearney G.J. Evaluation

of collagen in atherosclerotic plaques: the use of two coherent laser-based imaging methods. *Laser Med Sci* 2009 May; 24(3): 439–445.

20. Kubo T., Xu C., Wang Z., van Ditzhuijzen N.S., Bezerra H.G. Plaque and thrombus evaluation by optical coherence tomography. *Int J Cardiovasc Imag* 2011 Feb; 27(2): 289–298.

21. MacNeill B.D., Jang I.K., Bouma B.E., Iftimia N., Takano M., Yabushita H., Shishkov M., Kauffman C.R., Houser S.L., Aretz H.T., DeJoseph D., Halpern E.F., Tearney G.J. Focal and multi-focal plaque distributions in patients with macrophage acute and stable presentations of coronary artery disease. *J Am Coll Cardiol* 2004 Sep 1; 44(5): 972–979.

22. Tearney G.J., Yabushita H., Houser S.L., Aretz H.T., Jang I.K., Schlendorf K.H., Kauffman C.R., Shishkov M., Halpern E.F., Bouma B.E. Quantification of macrophage content in atherosclerotic plaques by optical coherence tomography. *Circulation* 2003 Jan 7; 107(1): 113–119.

23. Drexler W., Morgner U., Kartner F.X., Pitris C., Boppart S.A., Li X.D. In vivo ultrahigh-resolution optical coherence tomography. *Opt Lett* 1999; 24: 1221–1223.

24. Yabushita H., Bouma B.E., Houser S.L., Aretz T., Jang I.K., Schlendorf K.H., Kauffman C.R., Shishkov M., Kang D.H., Halpern E.F., Tearney G.J. Characterization of human atherosclerosis by optical coherence tomography. *Circulation* 2002 Sep 24; 106(13): 1640–1645.

25. Giattina S.D., Courtney B.K., Herz P.R., Harman M., Shortkroff S., Stamper D.L., Liu B., Fujimoto J.G., Brezinski M.E. Assessment of coronary plaque collagen with polarization sensitive optical coherence tomography (PS-OCT). *Int J Cardiol* 2006 Mar 8; 107(3): 400–409.

26. Kuo W.C., Chou N.K., Chou C., Lai C.M., Huang H.J., Wang S.S., Shyu J.J. Polarization-sensitive optical coherence tomography for imaging human atherosclerosis. *Applied Optics* 2007 May 1; 46(13): 2520–2527.

27. Nadkarni S., Pierce M., Park H., deBoer J., Houser S., Bressner J. Polarization-sensitive optical coherence tomography for the analysis of collagen content in atherosclerotic plaques. *Circulation* 2005; 112(17): 679.

28. Nadkarni S.K., Pierce M.C., Park B.H., de Boer J.F., Whittaker P., Bouma B.E., Bressner J.E., Halpern E., Houser S.L., Tearney G.J. Measurement of collagen and smooth muscle cell content in atherosclerotic plaques using polarization-sensitive optical coherence tomography. *J Am Coll Cardiol* 2007 Apr 3; 49(13): 1474–1481.

29. de Boer J.F., Milner T.E., van Gemert M.J., Nelson J.S. Two-dimensional birefringence imaging in biological tissue by polarization-sensitive optical coherence tomography. *Optics Letters* 1997 Jun 15; 22(12): 934–936.

30. Everett M.J., Schoenenberger K., Colston B.W., da Silva L.B. Birefringence characterization of biological tissue by use of optical coherence tomography. *Optics Letters* 1998 Feb 1; 23(3): 228–230.

31. de Boer J.F., Milner T.E. Review of polarization sensitive optical coherence tomography and Stokes vector determination. *J Biomed Optic* 2002 Jul; 7(3): 359–371.

32. Park B.H., Pierce M.C., Cense B., Yun S.H., Mujat M., Tearney G., Bouma B., de Boer J. Real-time fiber-based multi-functional spectral-domain optical coherence tomography at 1.3 microm. *Optics Express* 2005 May 30; 13(11): 3931–3944.

33. Park B.H., Saxer C., Srinivas S.M., Nelson J.S., de Boer J.F. In vivo burn depth determination by high-speed fiber-based polarization sensitive optical coherence tomography. *J Biomed Optic* 2001 Oct; 6(4): 474–479.

34. Saxer C.E., de Boer J.F., Park B.H., Zhao Y., Chen Z., Nelson J.S. High-speed fiber-based polarization-sensitive optical coherence tomography of in vivo human skin. *Optics Letters* 2000 Sep 15; 25(18): 1355–1357.

35. Zhang J., Jung W., Nelson J.S., Chen Z. Full range polarization-sensitive Fourier domain optical coherence tomography. *Optics Express* 2004 Nov 29; 12(24): 6033–6039.

36. Oh W.Y., Yun S.H., Vakoc B.J., Shishkov M., Desjardins A.E., Park B.H., de Boer J.F., Tearney G.J., Bouma B.E. High-speed polarization sensitive optical frequency domain imaging with frequency multiplexing. *Optics Express* 2008 Jan 21; 16(2): 1096–1103.

37. Suter M.J., Tearney G.J., Oh W.Y., Bouma B.E. Progress in intracoronary optical coherence tomography. *IEEE Selected Topics in Quantum Electronics* 2010 Jul–Aug; 16(4): 706–711.
38. Suter M.J., Nadkarni S.K., Weisz G., Tanaka A., Jaffer F.A., Bouma B.E., Tearney G.J. Intravascular optical imaging technology for investigating the coronary artery. *J Am Coll Cardiol Img* 2011; 4(9): 1022–1039.
39. Schmitt J.M., Xiang S.H. Cross-polarized backscatter in optical coherence tomography of biological tissue. *Optics Letters* 1998; 23(13): 1060–1062.
40. Feldchtein F., Gelikonov V., Iksanov R., Gelikonov G., Kuranov R., Sergeev A., Gladkova N., Ourutina M., Reitze D., Warren J. In vivo OCT imaging of hard and soft tissue of the oral cavity. *Optics Express* 1998 Sep 14; 3(6): 239–250.
41. Gladkova N., Streltsova O., Zagaynova E., Kiseleva E., Gelikonov V., Gelikonov G., Karabut M., Yunusova K., Evdokimova O. Cross polarization optical coherence tomography for early bladder cancer detection: statistical study. *J Biophotonics* 2011 Aug; 4(7–8): 519–532.
42. Gladkova N., Kiseleva E., Robakidze N., Balalaeva I., Karabut M., Gubarkova E., Feldchtein F. Evaluation of oral mucosa collagen condition with cross-polarization optical coherence tomography. *J Biophotonics* 2013 Apr; 6(4): 321–329.
43. Gladkova N., Kiseleva E., Streltsova O., Prodanets N., Snopova L., Karabut M., Gubarkova E., Zagaynova E. Combined use of fluorescence cystoscopy and cross-polarization OCT for diagnosis of bladder cancer and correlation with immunohistochemical markers. *J Biophotonics* 2013 Sep; 6(9): 687–698.
44. Gelikonov V.M., Gelikonov G.V. New approach to cross-polarized optical coherence tomography based on orthogonal arbitrarily polarized modes. *Laser Phys Lett* 2006; 3(9): 445–451.
45. Feldchtein F.I., Gelikonov V.M., Gelikonov G.V. *Polarization-sensitive common path optical coherence reflectometry/tomography device*. US patent 7,728,985 B2 2010 June 1.
46. Junqueira L.C., Bignolas G., Brentani R.R. Picrosirius staining plus polarization microscopy, a specific method for collagen detection. *J Histochem* 1979; 11: 447–455.
47. Stary H.C., Chandler A.B., Dinsmore R.E., Fuster V., Glagov S., Insull W.J., Rosenfeld M.E., Schwartz C.J., Wagner W.D., Wissler R.W. A definition of advanced types of atherosclerotic lesions and a histological classification of atherosclerosis: a report from the Committee on Vascular Lesions of the Council on Arteriosclerosis, American Heart Association. *Arterioscler Thromb Vasc Biol* 1995; 15: 1512–1531.
48. Rieber J., Meissner O., Babaryka G., Reim S., Oswald M., Koenig A., Schiele T.M., Shapiro M., Theisen K., Reiser M.F., Klauss V., Hoffmann U. Diagnostic accuracy of optical coherence tomography and intravascular ultrasound for the detection and characterization of atherosclerotic plaque composition in ex vivo coronary specimens: a comparison with histology. *Coron Artery Dis* 2006 Aug; 17(5): 425–430.
49. Kiseleva E.B., Gladkova N.D., Sergeeva E.A., Kirillin M.Yu., Gubarkova E.B., Karabut M.M., Balalaeva I.V., Streltsova O.S., Robakidze N.S., Maslennikova A.V., Kochueva M.V. *Sposob ocenki funkcionalnogo sostoyaniya tkani* [Method for evaluating the functional state of collagen tissue]. Zayavka na izobretenie №2013135571 ot 29.07.2013 [The application for the invention №2013135571 from 29.07.2013].